

plored. The numerically more difficult optimization of doublet shapes is now under investigation.

It is a pleasure to thank Gareth Guest, Don Dobrott, Fred McClain, and Wayne Pfeiffer for stimulating discussions, and Bob Davidson and Boni Dy for programming assistance. This work has been supported by the U. S. Department of Energy under Contract No. EY-76-C-03-0167, Project Agreement No. 38.

¹D. R. Dobrott *et al.*, in *Proceedings of the Seventh International Conference on Plasma Physics and Controlled Nuclear Fusion, Innsbruck, Austria 1978* (International Atomic Energy Agency, Vienna, Austria, 1978), Paper No. IAEA CN-37-P-4.

²M. S. Chance *et al.*, Ref. 1, Paper No. IAEA CN-37-P-2.

³R. A. Dory *et al.*, Ref. 1, Paper No. IAEA CN-37-K-1.

⁴C. Mercier, Ref. 1, Paper No. IAEA CN-37-P3-2.

⁵E. Rebhan and A. Salat, Nucl. Fusion **18**, 1639 (1978).

⁶D. R. Dobrott and R. L. Miller, Phys. Fluids **20**, 1361 (1977).

⁷Y.-K. M. Peng *et al.*, Phys. Fluids **21**, 467 (1978).

⁸L. C. Bernard *et al.*, General Atomic Company Report No. GA-A15236, December 1978 (to be published).

⁹D. R. Dobrott *et al.*, Phys. Rev. Lett. **39**, 943 (1977).

¹⁰J. W. Connor *et al.*, Phys. Rev. Lett. **40**, 396 (1978).

¹¹Yu. N. Yavlinskii, Nucl. Fusion **13**, 951 (1973).

¹²B. Coppi, private communication.

¹³D. Berger *et al.*, in *Proceedings of the Sixth International Conference on Plasma Physics and Controlled Nuclear Fusion Research, Berchtesgaden, West Germany, 1976* (International Atomic Energy Agency, Vienna, 1977), Vol. 2, p. 411.

¹⁴R. L. Miller, General Atomic Company Report No. GA-A15186, November 1978 (to be published).

Confinement of Fusion-Produced Tritium in the Princeton Large Torus

P. Colestock, J. D. Strachan, M. Ulrickson, and R. Chrien

Plasma Physics Laboratory, Princeton University, Princeton, New Jersey 08544

(Received 21 May 1979)

Tritium is produced in deuterium discharges in the Princeton Large Torus by the reaction $D(d, p)T$. These tritons undergo reactions $D(t, n)^4\text{He}$ creating 14-MeV neutrons which have been detected by two independent techniques at a level of 1% of the 2.5-MeV neutrons from the reaction $D(d, n)^3\text{He}$. The magnitude of the 14-MeV neutron emission is consistent with finite banana width, neoclassical predictions for the confinement of the energetic tritons.

A requirement for operation of an ignited fusion reactor is that the charged fusion reaction products be well confined since their energy is required to overcome the plasma energy losses. In this Letter, we report experimental evidence that such fusion reaction products are confined in a tokamak plasma [PLT (Princeton Large Torus)] consistent with finite-banana-width, neoclassical predictions.

In deuterium discharges, 1.01-MeV tritons are produced by the reaction $D(d, p)T$ with nearly equal probability as the 2.45-MeV ($d-d$) neutrons produced by the reaction $D(d, n)^3\text{He}$. A fraction of the tritons may then react further to produce 14-MeV ($d-t$) neutrons by the reaction $D(t, n)^4\text{He}$. The ratio of $d-t$ to $d-d$ neutrons produced in a given discharge is strongly dependent on the confinement of the tritons as they slow down from 1.01 MeV through the maximum of the $D(t, n)^4\text{He}$ cross section near 170 keV. About 10^{-2} of the confined tritons undergo reactions $D(t, n)^4\text{He}$. Unconfined tritons still encounter deuterium in the vacuum vessel wall,¹ but due to the shorter triton

slowing-down time in the metal, only about 10^{-6} undergo reactions $D(t, n)^4\text{He}$. The $d-t/d-d$ neutron flux ratio of about 1/100 observed on PLT is thus an indication that the tritons have been confined during most of their slowing-down time.

In these experiments, PLT (500 kA, 3.2 Tesla, 40 cm minor radius, and 130 cm major radius)² was heated by hydrogen or deuterium neutral-beam injection (37 keV, 1.4 MW)³ into a deuterium target plasma resulting in plasma conditions of $n_e(0) = 4 \times 10^{13} \text{ cm}^{-3}$, $T_e(0) = 2 \text{ keV}$, $T_i(0) \approx 2 \text{ keV}$. The Thomson scattering⁴ deduced electron temperature profile during neutral-beam injection indicated a highly peaked $T_e(r)$ profile similar to $[1 - (r/a)^2]$.⁴ The Z_{eff} was about 3, and spectroscopic observations indicated that the main impurity was carbon. As a result of the neutral-beam injection, the neutron emission rate rose from about 10^8 to 10^{11} per second for H^0 injection and to 10^{12} per second for D^0 injection.

The 14-MeV neutron flux was measured with two independent systems. The first was a 13-cm \times 13-cm-diam NE213 liquid scintillator in which

incident neutrons induce recoil protons. The neutron spectrum may then be derived from the proton recoil spectrum. This system has the advantage of being able to directly measure the neutron spectra. The scintillator was situated in a collimator which was aligned tangential to the plasma current. Collimation was achieved using Li_2CO_3 +paraffin shield with a conical aperture⁵ and a 10-cm Pb shield surrounding the detector to reduce the γ -ray background. γ -ray counts were further reduced by pulse shape discrimination based on standard crossover timing techniques.⁶ The energy calibration was determined with use of accelerator-produced 3- and 16-MeV neutron beams as well as a ^{22}Na Compton electron light unit.⁶ The energy resolution was determined to be about 10% at 2.5 MeV. The ratio of d - d to d - t neutrons is derived from the recoil proton edges in the pulse-height spectrum at 2.5 and 14 MeV (Fig. 1). The d - t / d - d ratio is the product of the ratios of the recoil proton counts per unit energy, the neutron-scattering cross sections, and the collimator aperture at the two energies. The use of a collimated neutron spectrometer to measure both d - d and d - t neutrons reduced the proportion of scattered neutrons and provides a definite detector-plasma geometry.

During hydrogen neutral-beam injection, the d - t / d - d neutron ratio was found to be about 1/200 with 500 kA (Fig. 2) and 1/300 with 250-kA plasma current. The prime uncertainty is the wider

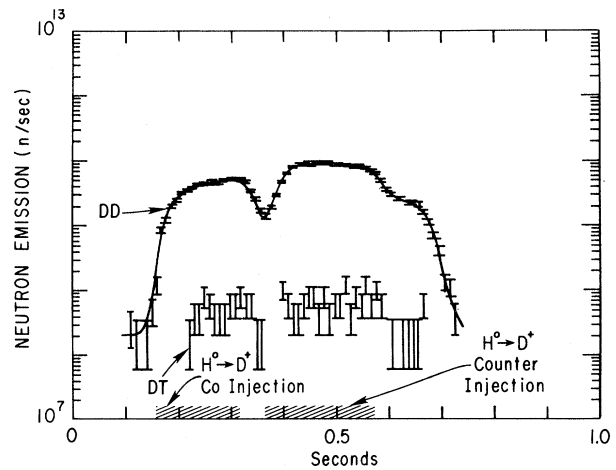


FIG. 2. Time evolution of the 14-MeV neutron emission with $\text{H}^0 \rightarrow \text{D}^+$ injection as measured with the NE213 scintillator.

effective collimator aperture for 14-MeV neutrons than for 2.5-MeV neutrons due to the approximately three-times-longer scattering length in the conical collimator aperture. The energy dependence of the aperture width was estimated at 3 and 8 MeV with use of a PuBe source and extrapolation to 14 MeV. This procedure may underestimate the magnitude of the d - t emission by a factor of 2. The measured width of the 2.5-MeV line is entirely instrumental while the width of the 14-MeV line is limited in accuracy by count-

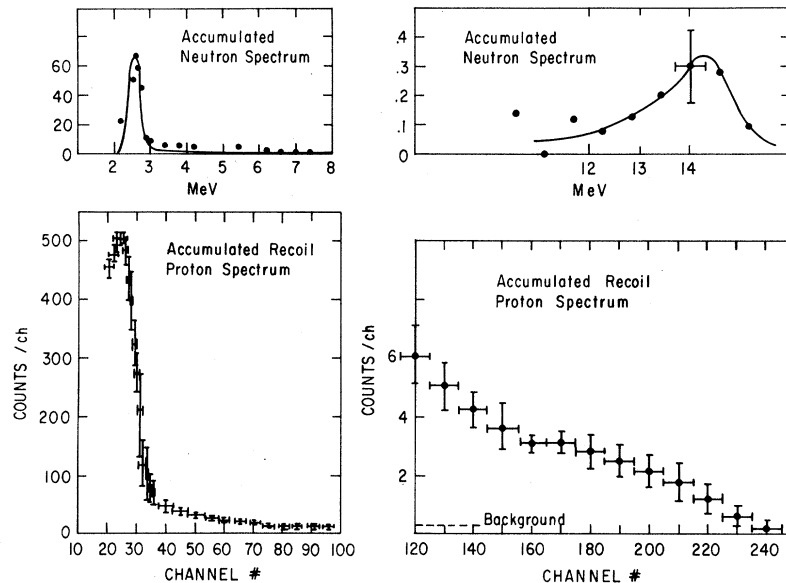


FIG. 1. Proton recoil spectrum of the NE213 scintillator showing the 2.5- and 14-MeV recoil edges. Unfolded pulse-height spectrum showing peak at 2.5 and 14 MeV in the ratio of about 200/1.

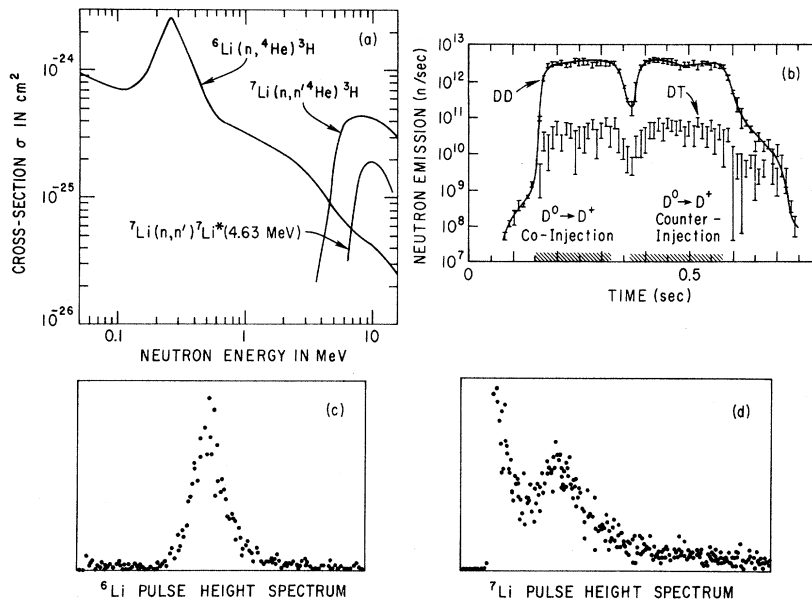


FIG. 3. (a) Cross sections for the reactions ${}^6\text{Li}(n, \alpha)\text{T}$ (NE912 scintillator) and ${}^7\text{Li}(n, n'\alpha)\text{T}$ (NE913 scintillator) used in the glass scintillators. The ${}^6\text{Li}$ scintillator responds mainly to low-energy neutrons and is responsive to the $d-d$, 2.5-MeV neutrons. The ${}^7\text{Li}$ scintillator responds to incident neutrons with energies above 5 MeV and therefore only the $d-t$, 14-MeV neutrons. (b) Time evolution of the $d-d$ and $d-t$ neutron emission for the case of $\text{D}^0 \rightarrow \text{D}^+$ injection as measured by the glass scintillators. (c) ${}^6\text{Li}$ pulse-height spectrum showing the peak associated with the positive Q of the ${}^6\text{Li}$ reaction, and primarily due to the $d-d$ neutrons. (d) The ${}^7\text{Li}$ scintillator pulse-height spectrum showing a peak due to the 4.63-MeV excited level produced by $d-t$ neutrons.

ing statistics. The 2.5-MeV line is expected to be about 0.15 MeV wide, and the width at 14 MeV can be about 2.5 MeV wide due to the high velocity of the triton.

The second method of measuring the $d-t$ neutron emission used a pair of 2.5-cm \times 2.5 cm lithium glass scintillators, one of which contained high-purity ${}^7\text{Li}$ (NE913) and the other contained enriched ${}^6\text{Li}$ (NE912). The reaction ${}^7\text{Li}(n, n'\alpha)\text{T}$ produces a peak in the scintillator pulse-height spectrum [Fig. 3(d)] when it proceeds through the 4.6-MeV excited level of ${}^7\text{Li}$. This reaction has a threshold [Fig. 3(a)] of 5.3 MeV, thereby discriminating against $d-d$ neutrons. The ${}^6\text{Li}$ scintillator uses the exoergic reaction ${}^6\text{Li}(n, \alpha)\text{T}$ [Fig. 3(a)] and measures the $d-d$ emission, which is also measured with moderated BF_3 counters. The ${}^6\text{Li}$ impurity in the ${}^7\text{Li}$ scintillator was measured to be 0.1% with use of 2 keV, filtered reactor neutrons.⁷ Typical ${}^6\text{Li}$ and ${}^7\text{Li}$ pulse-height spectra are shown in Figs. 3(c) and 3(d).

The ratio of $d-t/d-d$ neutrons was determined to be 1/150 from the ratio of ${}^7\text{Li}/{}^6\text{Li}$ scintillator counts divided by the ratio of the reaction cross sections (${}^7\text{Li}$ at 14 MeV/ ${}^6\text{Li}$ at 2.5 MeV) [Fig. 3(a)]. This is expected to underestimate the $d-t/$

$d-d$ ratio since the ${}^6\text{Li}$ cross section [Fig. 3(a)] rises strongly for low-energy neutrons such as neutrons whose energies have been degraded by scattering. A factor-of-2 uncertainty is introduced by the background [Fig. 3(d)] which must be subtracted from the ${}^7\text{Li}$ peak.

The predicted fraction of confined tritons was determined by a Monte Carlo code⁸ which followed the guiding center orbits of 10^3 tritons generated from the triton birth distribution with random pitch angles. The tritons are essentially all born near the plasma center (inside 15 cm).⁹ Most of the unconfined tritons are born in loss regions. Pitch-angle scattering acts principally to spread the trajectories causing the tritons to sample a large portion of the plasma volume. The tritons slow down mostly on electrons. Effects due to ion drag, impurities, toroidal electrical fields, and energy diffusion were also considered but do not have a major influence on the results. The confined fraction is a strong function of the plasma current inside the drift orbits ($r \leq 25$ cm) since the poloidal magnetic field determines the minimum loss energy. For these PLT discharges the confined fraction is predicted to be 70% at the plasma center (Fig. 4). The average over

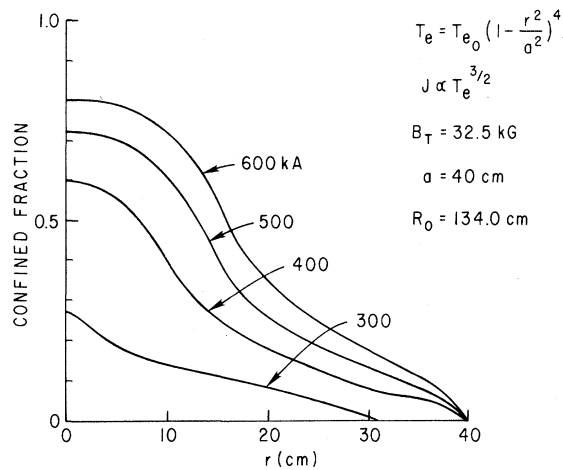


FIG. 4. Predicted fraction of confined tritons as a function of radius for several values of total discharge current. The confinement of tritons born within 15 cm of the center is a strong function of the current inside about 25 cm.

the birth distribution indicated about 50% total confinement.

The probability of fusion for each triton was determined along its guiding-center orbit. Since the tritons are born with 1.01 MeV of energy, they actually slow down through the maximum of the $d-t$ reaction cross section and undergo essentially all their fusion reactions while they have energies greater than 80 keV. The burnup of the confined tritons is about 1.0%, indicating a $d-t/d-d$ ratio of about 1/250, which is within the experimental uncertainties of the measured values. However, the probability of any unconfined triton undergoing a $d-t$ fusion reaction is $\sim 10^{-6}$ based on the deuterium content of the vacuum vessel¹ and the range of a 1-MeV triton. Tritium contamination is not detectable by the PLT mass spectrometer nor from tritium retention measurements¹⁰ in the vacuum walls. It is thus over two orders of magnitude below the contamination levels required to explain the $d-t$ neutron observations.

The experimental results are summarized as follows. The NE213 scintillator was used to measure the $d-t$ neutron emission from deuterium discharges heated by hydrogen neutral injection, $H^0 \rightarrow D^+$, resulting in a $d-d$ neutron emission level of $\sim 10^{11}$ per second. The $d-t/d-d$ neutron ratio was about 1/200 at $I_p = 500$ kA (Fig. 2) and 1/300 at $I_p = 250$ kA. The ^7Li glass scintillator was used to measure the $d-t$ neutron emission from deuterium discharges with deuterium in-

jection, $D^0 \rightarrow D^+$, resulting in a $d-d$ neutron emission level of $\sim 2 \times 10^{12}$ per second. The $d-t/d-d$ neutron ratio was found to be 1/150 [Figs. 3(b) and 3(d)]. The NE 213 detector saturated at the higher emission levels associated with deuterium injection, while the ^7Li glass scintillator was not sufficiently sensitive to detect the lower $d-t$ emission levels from hydrogen injection. Since the triton confinement code predicted about 50% triton confinement with a $d-t/d-d$ ratio of 1/250, the tritons are confined in PLT during most of their slowing-down time. The observed change in the $d-t/d-d$ ratio with plasma current is consistent with the expected scaling of the triton confinement (Fig. 4).

The time evolution of the $d-t$ neutron emission [Figs. 2 and 3(b)] indicates little difference between $H^0 \rightarrow D^+$ and $D^0 \rightarrow D^+$ injection in either same or opposite directions. This is consistent with the Monte Carlo code model. Since the counts in a single time interval are a small fraction of the total counts [Fig. 2(b)], the statistics are relatively poor and preclude detailed analysis of the time dependence.

We take the agreement between the experimentally observed $d-t/d-d$ neutron ratio in two different cases by two independent methods to indicate that the tritons are confined during most of their slowing down time. PLT is the first tokamak device with sufficient plasma current to confine these energetic tritons. The triton confinement is marginal, however, and the higher-energy fusion reaction products (protons and alphas) are expected to be poorly confined.

The authors thank W. Stodiek with the PLT experimental team, H. Eubank with the PLT neutral-beam injection team, and J. Hovey for help in performing these measurements. Helpful discussions with R. Goldston, D. Jassby, G. Morgan, and D. Slaughter are gratefully acknowledged. The authors are also grateful to K. R. Jones and R. E. Chrien of Brookhaven National Laboratory for assistance in calibrating the detectors. This work was supported by the U. S. Department of Energy Contract No. EY-76-C-02-3073.

¹H. F. Dylla, *J. Nucl. Mater.* **76 & 77**, 459 (1978).

²D. Grove *et al.*, in *Proceedings of the Sixth International Conference on Plasma Physics and Controlled Nuclear Research, Berchtesgaden, West Germany, 1976* (International Atomic Energy Agency, Vienna, 1977), Vol. 1, p. 21.

³H. Eubank *et al.*, in *Proceedings of the Seventh Inter-*

national Conference on Plasma Physics and Controlled Nuclear Research, Innsbruck, Austria, 1978 (International Atomic Energy Agency, Vienna, Austria, 1979), and Princeton Plasma Physics Laboratory Report No. 1491, 1978 (unpublished).

⁴N. Bretz *et al.*, *Appl. Opt.* **17**, 192 (1978).

⁵D. Glasgow *et al.*, *Nucl. Instrum. Methods* **114**, 521 (1974).

⁶W. R. Burrus and V. V. Verbinski, *Nucl. Instrum.*

Methods **67**, 125 (1969).

⁷R. C. Greenwood and R. E. Chrien, *Nucl. Instrum. Methods* **138**, 125 (1976).

⁸D. L. Jassby and R. J. Goldston, *Nucl. Fusion* **16**, 613 (1976).

⁹J. D. Strachan *et al.*, *Phys. Lett.* **66A**, 295 (1978).

¹⁰W. R. Wampler *et al.*, to be published, and in *Proceedings of the First Topical Meeting on Fusion Reactor Materials*, Miami, Florida, 1979 (to be published).

Surface-Enhanced Raman Spectroscopy and Surface Plasmons

J. C. Tsang, J. R. Kirtley, and J. A. Bradley

IBM Thomas J. Watson Research Center, Yorktown Heights, New York 10598

(Received 3 July 1979)

The Raman spectra of 4-pyridine-carboxaldehyde-doped Al-Al₂O₃-Ag tunnel junctions evaporated onto CaF₂ films and optical diffraction gratings show that the molecular Raman scattering is strongly enhanced under conditions which permit the direct excitation of the surface plasmon modes of Ag. This suggests that the surface plasmon is an intermediate state in surface-enhanced Raman scattering.

The ability of conventional Raman spectroscopy to observe the vibrational modes of a molecular monolayer adsorbed on a metal surface has recently been established.¹⁻³ This result implies an enormous enhancement ($\sim 10^6$) of the Raman cross section for the adsorbed molecules over that for the same molecules in solution, and has attracted considerable experimental and theoretical interest.⁴⁻⁶ However, the mechanism for these enormous enhancements remains unknown.⁶

We have previously shown that surface-enhanced Raman (SER) scattering can be observed for 4-pyridine-carboxaldehyde (4-py-COH) adsorbed onto the oxide surface of an Al-Al₂O₃-(4-py-COH)-Ag tunneling junction structure.³ Combined measurements of the SER scattering and the inelastic electron tunneling spectra of these samples allowed us to confirm the existence of SER scattering in this non-electrolytic-cell system and show that SER scattering is both molecule and metal selective. In this paper, we report on a detailed study of the coupling of light to the vibrational excitations of 4-py-COH in this system. We present quantitative results on the dependence of the intensity of the SER scattering on surface roughness, laser excitation energy and the angle of incidence, and polarization of the exciting light for samples evaporated on rough CaF₂ films and a diffraction grating. Our results strongly suggest that the SER scattering process on Ag can proceed through the surface plasmon of Ag as an intermediate state.

All of our measurements were made on molecular monolayers chemisorbed on the oxide grown on evaporated Al films and then covered with 20 nm of silver. The samples were evaporated either on different thicknesses of CaF₂ or on a 1200-line/mm diffraction grating. The measurements were performed at 300 K and low levels of laser power to eliminate the possibility of laser-induced damage to the sample. Lines from both Kr⁺ and Ar⁺ lasers were used and the Raman spectra were collected over a solid angle of $\sim 90^\circ$ and analyzed by a double monochromator.

In Fig. 1 we show the Raman spectra of three Al-Al₂O₃-(4-py-COH)-Ag structures evaporated on different thicknesses of CaF₂. Metallic films evaporated on 10- to 100-nm-thick layers of CaF₂ have been shown to be rougher than films evaporated directly onto microscope slides.⁷ The rms magnitude of the surface roughness increases film thickness, reaching a value of 3 to 4 nm for a 100-nm thick CaF₂ film.⁷ In Fig. 1, we show that the intensity of the SER scattering from the 4-py-COH increases monotonically with increasing CaF₂ thickness. Radioactive-tracer studies using similarly prepared structures doped with benzoic acid show that the introduction of a roughened surface produces a change in the density of adsorbed molecules of less than a factor of 3, i.e., only a small part of the observed intensity change. In Fig. 2, we show the dependence on CaF₂ thickness of the intensity of the Raman mode at 1610 cm⁻¹. In Fig. 2, we also show the results of